

# Experimental Observation and Numerical Simulation of Initiation and Propagation of Compaction Bands in a Sandstone

Veronika Vajdova<sup>1</sup>, Teng-fong Wong  
David E. Farrell, Kathleen A. Issen<sup>2</sup> and Vennela Challa

## ABSTRACT

Recent field, laboratory and theoretical studies have confirmed the occurrence of strain localization in porous sandstones in the forms of conjugate shear or compaction bands oriented subperpendicular to the maximum compression direction in the transitional regime from brittle faulting to cataclastic flow. Some field observations show that compaction bands develop in the vicinity of local stress concentration. As an analogue of this phenomenon, we conducted triaxial compression tests on circumferentially notched samples of Bentheim sandstone at confining pressure of 300 MPa. The sample configuration was similar to that used in fracture mechanics tests, but with the maximum compressive stress instead of tensile. Our mechanical data show that the nominal yield stress for a notched sample was lower than for an intact sample, and the onset of compactive yield was marked by enhancement of acoustic emission activity. Microstructure of deformed samples shows incremental growth of the bands from the notch tip along a direction perpendicular to the maximum compressive stress. Increasing axial strain is accommodated by development of a subparallel array of localized cataclastic bands. Computational analysis was performed using a Drucker-Prager with cap constitutive model. Results confirm that a stress concentration exists at the notch, which causes a stress state favoring axial compaction perpendicular to the maximum compressive stress. However, to reproduce compaction band propagation, further refinement of the model is required.

## INTRODUCTION

Compaction localization has been described in field (Mollema and Antonellini, 1996) and laboratory (Olsson, 1999; DiGiovanni et al., 2000; Olsson and Holcomb, 2000; Baud et al., 2003) studies as an important failure mode in compacting porous sandstone. In tectonic settings the coupled development of compaction and strain localization may significantly impact the stress field, strain partitioning and fluid transport and therefore better understanding of how such localizations develop is desirable. Laboratory studies on Bentheim sandstone performed by Wong et al. (2001) and Baud et al. (2003) documented that compaction can localize in discrete bands normal to  $\sigma_1$  direction at stresses associated with the transition from brittle faulting to cataclastic flow and suggested the importance of local stress heterogeneity for compaction bands development. Local heterogeneities are pervasive at all scales, and a deeper understanding of how they control the initiation of compaction localization necessitates studying the process under well-defined conditions of stress concentration.

To investigate compaction band initiation and propagation from a stress concentration, we combined an experimental approach with microscopy observations and finite element modeling. We conducted triaxial compression experiments on cylindrical samples of Bentheim sandstone with a circumferential notch in its midsection. While such a sample configuration has been widely used for studying tensile fracture, we are not aware of similar studies in compression. The finite element modeling was conducted with the ABAQUS software package using the Drucker-Prager with cap constitutive relation, appropriate for pressure sensitive geomaterials.

## EXPERIMENTAL DATA AND RESULTS

The Bentheim sandstone samples (with porosity of 23% and average grain diameter of 0.21 mm) were cored perpendicular to the sedimentary bedding, with diameter  $D = 18.4$  mm and length 38.1 mm. A V-shaped notch (2 mm deep and 2 mm wide) was machined along the circumference of the mid-section of

---

<sup>1</sup> State University of New York at Stony Brook, Stony Brook, NY, 11794-2100; vvajdova@ic.sunysb.edu

<sup>2</sup> Clarkson University, Mech. & Aero. Engr., Potsdam, NY, 13699-5725; issenka@clarkson.edu

the sample (Fig. 1a). The minimum diameter was  $d = 14.4$  mm. The mechanical and acoustic emission (AE) measurements were conducted in the conventional triaxial configuration (with the compressive principal stresses given by  $\sigma_1 > \sigma_2 = \sigma_3$ ) following methodology detailed previously (Wong *et al.*, 1997; Baud *et al.*, 2003). The notched sample was jacketed with a thin copper foil and then with polyolefine tubing. The nominally dry samples were deformed at confining pressure  $P_c = 300$  MPa, and the axial displacement was servo-controlled at a rate of  $0.5 \mu\text{m/s}$ . After accounting for the elastic deformation of the loading system and normalizing the sample displacement by the nominal length, this fixed displacement rate corresponds to a nominal axial strain rate of  $1.0 \times 10^{-5} \text{ s}^{-1}$ . To study the micromechanics of the compaction band formation experiments were stopped at different stages of axial shortening and the samples were retrieved from the pressure vessel for microstructural observations using optical microscopy (Fig. 1a).

In loading an unnotched specimen (Klein *et al.*, 2001) differential stress,  $\sigma_1 - \sigma_3$ , first attained a peak and then the overall strain hardening trend was punctuated by episodic stress drops with concomitant surges in AE activity. For notched specimens the results of selected mechanical experiments summarized in Fig. 1b-c show qualitatively similar behavior. The samples were loaded to three stages of deformation characterized in Fig. 1b by: 1) increase of AE rate above background level (sample BN7), 2) attaining a peak stress (BN5) and 3) loading past several stress drops (BN1). The confining pressure was applied first to the notched jacketed sample using liquid pressure medium, then additional axial force was applied at the ends of the sample. We can normalize this additional force by the sample end area to obtain “nominal differential stress”. Microscopy confirmed that localized damage is qualitatively similar for both notched and unnotched cases in that the compaction band is a planar zone normal to  $\sigma_1$  of significant grain crushing extending over a width of 2-3 grains. Relatively less damage was observed in areas outside the discrete bands. While for the unnotched sample the bands develop as an array close to the ends of the sample, in the notched experiments the localized damage was observed to initiate and propagate only in the sample’s midsection (Fig. 1c). The compaction band was observed to initiate at the notch tip and with further strain to propagate inwards.

## FINITE ELEMENT SIMULATION

The finite element simulation was conducted with the commercial software package, ABAQUS<sup>®</sup>. Isotropic elasticity with constant elastic moduli was assumed. The Drucker-Prager with cap constitutive

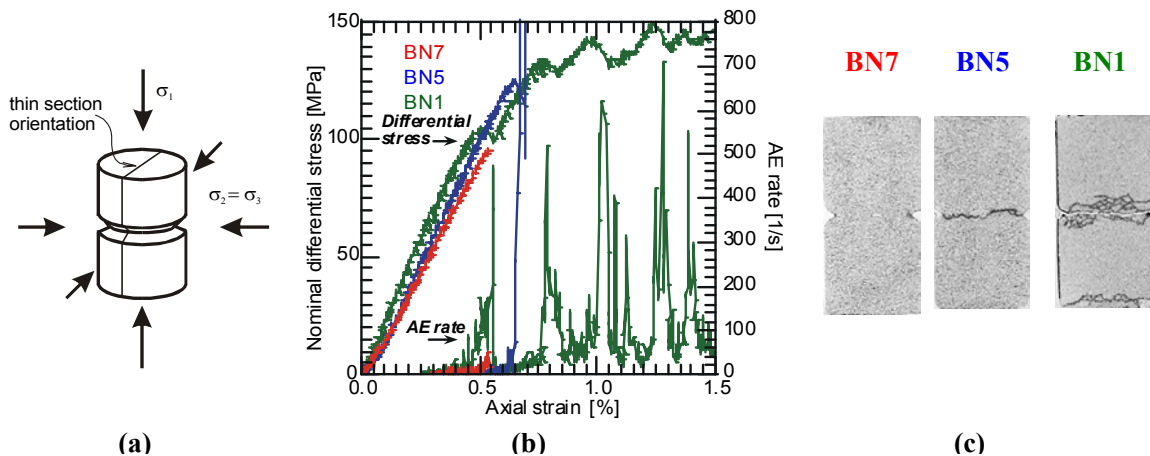


**Fig. 1** a) Notched sample configuration in conventional triaxial compression. b) Experimental results for three selected notched samples loaded to different stages of triaxial deformation showing nominal differential stress and AE rate as a function of axial strain. c) Photographs of thin sections of the samples showing initiation and propagation of compaction bands as axial strain accumulates. (The sample BN1 broke apart when retrieved from the pressure vessel causing a white artifact line to appear in the thin section.)

model (ABAQUS Theory Manual) was used for the inelastic response. This model is characterized by a single yield surface in the stress space (see Fig. 2a). At low confining pressures, the “shear yield” portion of the surface,  $F_1 = Q - P \tan(\mu) - d = 0$ , corresponds to dilatant behavior. At higher confining pressures, the “cap” portion,  $F_2 = \sqrt{(P - P_a)^2 + R^2 Q^2 / (1 + \alpha - \alpha / \mu)^2} - R[d + P_a \tan(\mu)] = 0$ , corresponds to compactive behavior. The surfaces meet smoothly (no vertex) via a smoothing parameter,  $\alpha$ . Non-associated flow is used on the shear yield and transition portions, while associated flow is employed on the cap. The single plastic potential,  $\Gamma = \sqrt{(P - P_a)^2 \tan(\mu)^2 + Q^2 / (1 + \alpha - \alpha / \mu)^2}$ , is coincident with the cap at higher mean stresses. The differential stress is  $Q = \sigma_1 - \sigma_3$ , the mean stress is  $P = (\sigma_1 + \sigma_2 + \sigma_3)/3$ , the intercept of the yield surface on the  $Q$  axis is  $d = 50$  MPa, and the shear yield surface slope is  $\mu = 31.139^\circ$ . The eccentricity parameter,  $R = 0.8718$  describes the ratio of the major and minor axes of the elliptical cap ( $L_2/L_1$  in Fig. 2a) and  $P_a = 240$  MPa is the ellipse center. These parameters were determined from mechanical data for unnotched Bentheim axisymmetric compression tests (P. Baud, personal communication, 2002). Isotropic hardening was assumed for the post yield behavior. Simulation and experimental stress-strain curves for intact specimens at higher confining pressures were similar.

The model geometry is identical to the physical specimen. The loading conditions and boundary conditions (frictionless at upper and lower edges) simulate experiments. An axisymmetric model was used with a higher density mesh grid around the notch. For the notched simulations, distinct compressive axial stress and strain concentrations occurred at the notch tip (see Fig. 2b-c). In  $Q - P$  stress space, the loading path of the material near the sample end is steeper than that of material at the notch tip (see Fig. 2a). This corresponds to more negative values of  $\mu = \beta$  at the notch tip, which implies increased inelastic compactive volume strain, as seen experimentally.

The compactive axial stress and strain concentrations at the notch tip seem to provide conditions favorable for compaction bands to propagate radially inward from the notches. However, no compaction bands formed in the simulation. Several possible explanations for this discrepancy are offered. Fine-tuning of key parameter values for the single yield surface model employed here may be required. Alternatively, a two yield surface model may be required to represent the complex behavior of high porosity sandstone (Wong et al., 2001; Issen, 2002). If compaction band formation is viewed as a bifurcation from homogenous deformation (Olsson, 1999), then special computational procedures may be needed to simulate formation. Similarly, if a compaction band is viewed as an anti-crack (zone of

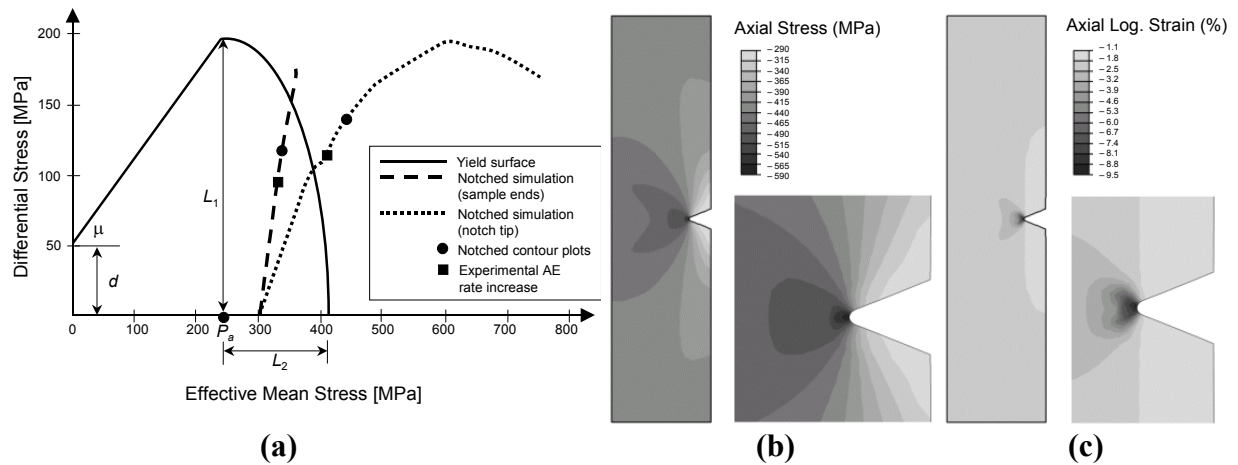


**Fig. 2** a) Initial yield surface used in the finite element model. The two loading paths refer to a triaxial loading simulation (confining pressure of 300 MPa) of a notched specimen. The steeper path is the stress state at the sample ends. The flatter path is the stress state at the notch tip. The square and circle markers identify two specific stages in axial shortening. b-c) Axial stress and axial strain distributions for the simulated sample loaded to overall axial strain of 0.7% (corresponding to circle markers on Fig. a). Notch tip is shown in detail.

propagating crack closure), special computation procedures may be required. Finally, improper simulation boundary conditions may inhibit localized band formation (Albert and Rudnicki, 2001).

## DISCUSSION AND SUMMARY

The two loading paths at Fig. 2a describe a notched experiment, one path representing stresses at a sample's end while the other at the notch tip. It can be seen that the material at the notch tip undergoes higher stress and that indeed the notch serves as a stress concentrator. Due to this concentration the material at the notch tip reaches the limit of linear elasticity (the yield cap) before the rest of the sample. The mechanical testing in conjunction with microstructure observations (Fig. 1b-c) revealed that onset of plastic deformation is associated with AE rate increase and fracturing at the notch tip. The stress state corresponding to this onset of plasticity (experimental AE increase) is superposed over the simulations as square markers at Fig. 2a. It is encouraging that this point appeared very close to where the simulated loading path for the notch tip hit the yield envelope. Loading beyond this point is no longer governed by linear elasticity and complications associated with hardening law are introduced. Circle markers at both loading paths refer to stage of deformation detailed further at Fig. 2b-c where simulated stress and strain are shown, respectively. Although stress concentration was confirmed by the simulation, the strain distribution does not indicate any compaction band. Accumulation of the strain at the notch tip (Fig. 2c) would be geometrically similar to damage observed at compaction band initiation at much lower stresses in sample BN7 at Fig. 1c. The comparison between the experiment and simulation suggests that favorable conditions exist for formation and radially inward propagation of compaction bands between notches but model refinement is necessary especially with respect to the post yield behavior.

## ACKNOWLEDGEMENTS

The authors would like to acknowledge financial support from the National Science Foundation, Directorate for Geosciences, Division of Earth Sciences (grant EAR-0106932 to Clarkson University and grant EAR-0106580 to State University of New York at Stony Brook).

## REFERENCES

- ABAQUS Theory Manual*, Hibbitt, Karlsson and Sorensen, Inc., v. 6.3-1 Online Documentation, 2002.
- Albert RA and JW Rudnicki, Finite element simulations of Tennessee marble under plane strain laboratory testing: Effects of sample-platen friction on shear band onset, *Mech. Mater.*, 33, 47-60, 2001.
- Baud P, E Klein and T-f Wong, Compaction localization in porous sandstones: Spatial evolution of damage and acoustic emission activity, *J. Struct. Geol.*, submitted, 2003.
- DiGiovanni AA, JT Fredrich, DJ Holcomb and WA Olsson, Micromechanics of compaction in an analogue reservoir sandstone, *Proceedings of the North American Rock Mechanics Symposium*, July 2000, 1153-1158, Ed. J Girard, M Liebman, C Breeds, T Doe, AA, Pub. AA Balkema, 2000.
- Issen KA, The influence of constitutive models on localization conditions for porous rock, *Eng. Fract. Mech.*, 69, 1891-1906, 2002.
- Klein, E, P Baud, T Reuschlé, T-f Wong, Mechanical Behaviour and Failure Mode of Bentheim Sandstone Under Triaxial Compression, *Phys. Chem. Earth (A)*, 26 (1-2), 21-25, 2001.
- Mollema PN and MA Antonellini, Compaction bands: a structural analog for anti-mode I cracks in Aeolian sandstone, *Tectonophysics*, 267, 209-228, 1996.
- Olsson WA, Theoretical and experimental investigation of compaction bands, *J. Geophys. Res.*, 104, 7219-7228, 1999.
- Olsson WA and DJ Holcomb, Compaction localization in porous rock, *Geophys. Res. Lett.*, 27(21), 3537-3540, 2000.
- Wong T.-f., P Baud and E Klein, Localized failure modes in compactant porous rock, *Geophys. Res. Lett.*, 28(13), 2521-2524, 2001.
- Wong T-f, C David and W Zhu, The transition from brittle faulting to cataclastic flow in porous sandstones: mechanical deformation, *J. Geophys. Res.*, 102(B2), 3009-3025, 1997.